Visualization of astaxanthin localization in HT29 human colon adenocarcinoma cells by combined confocal resonance Raman and fluorescence microspectroscopy

Karlis Briviba[1], Rainer Bornemann[2] and Ulrich Lemmer[2]

[1] Institute of Nutritional Physiology, Federal Research Centre for Nutrition, Karlsruhe, Germany
[2] Lichttechnisches Institut and Center for Functional Nanostructures, Universität Karlsruhe (TH), Karlsruhe, Germany

Astaxanthin, a carotenoid found in plants and seafood, exhibits antiproliferative, antioxidant and anti-carcinogenic properties. We show that astaxanthin delivered with tetrahydrofuran is effectively taken up by cultured colon adenocarcinoma cells and is localized mostly in the cytoplasm as detected by confocal resonance Raman and broad-band fluorescence microspectroscopy image analysis. Cells incubated with β-carotene at the same concentration as astaxanthin (10 μM) showed about a 50-fold lower cellular amount of β-carotene, as detected by HPLC. No detectable Raman signal of β-carotene was found in cells, but a weak broad-band fluorescence signal of β-carotene was observed. β-Carotene, like astaxanthin, was localized mostly in the cytoplasm. The heterogeneity of astaxanthin and β-carotene cellular distribution in cells of intestinal origin suggests that the possible defense against reactive molecules by carotenoids in these cells may also be heterogeneous.

Keywords: Adenocarcinoma cells / Astaxanthin / β-Carotene / Confocal fluorescence and resonance Raman microspectroscopy

Received: April 12, 2006; revised: July 27, 2006; accepted: July 29, 2006

1 Introduction

It has been suggested that some phytochemicals such as carotenoids may be responsible for the observed reduction in the risk of cardiovascular diseases and cancer after increased consumption of plant food [1 – 3]. This hypothesis is supported by *in vitro* and *in vivo* experiments showing that carotenoids, such as astaxanthin, scavenge and quench reactive oxygen species, inhibit proliferation of cancer cells, neoplastic cell transformation, up-regulate gap junction intercellular communication, suppress chemically-induced carcinogenesis in experimental animals, and exhibit anti-inflammatory effects [4 – 9]. Cultured cells are often used to investigate the molecular mechanisms of carotenoids [9, 10]. To investigate the efficacy of cellular uptake of carotenoids, extraction with subsequent determination of carotenoids by HPLC is widely used [11, 12]. Confocal Raman microspectroscopy is a noninvasive method that makes it possible to detect carotenoids like astaxanthin [13]. Here, we used a broad-band microfluorescence and a confocal resonance Raman microspectroscopy imaging approach to investigate the subcellular localization of astaxanthin in cultured colon adenocarcinoma cells.

Correspondence: Dr. Karlis Briviba, Institute of Nutritional Physiology, Federal Research Centre for Nutrition and Food, Haid-und-Neu-Str. 9, 76131 Karlsruhe, Germany
E-mail: karlis.briviba@bfel.de
Fax: +49-721-6625-404

2 Materials and methods

2.1 Chemicals

Unless otherwise stated, all chemicals were purchased from Merck (Darmstadt, Germany). DMEM, penicillin, streptomycin and PBS without Mg^{2+} and Ca^{2+} were purchased from Life Technologies (Eggenstein, Germany). Fetal calf serum (FCS) was obtained from Roche (Mannheim, Germany). Astaxanthin and β-carotene were from Sigma Chemical (Deisenhofen, Germany).

2.2 Cell culture and HPLC analysis of carotenoids

Human colon carcinoma cell line HT29 was purchased from DSZM (Braunschweig, Germany). Cells were maintained as described previously [11]. Three days after seeding the cells were incubated with cell culture medium sup-

plemented with astaxanthin or β-carotene. Carotenoids were extracted and determined by reversed-phase HPLC as described in reference [11].

2.3 Confocal resonance Raman and broad-band fluorescence microspectroscopy

The cells were treated with carotenoids as described above. After incubation, the cells were washed in PBS, fixed with methanol for 10 min at room temperature and washed again in PBS buffer. Raman measurements were carried out using a confocal Raman microspectrometer as described in [14]. Briefly, laser radiation of 532 nm with 25 mW from a cw diode pumped solid state (DPSS) laser (Coherent Verdi V10, Coherent, USA) was focused on the sample under investigation by a high numerical microscope objective (NA = 1.4, Nikon, Japan). Emission from the sample was collected by the same objective, filtered by a band-pass filter (AHF Analysentechnik, Germany) to suppress the reflected laser light and coupled into a spectrograph (TRIAX 320, HORIBA Jobin Yvon, Germany) which was used for the spectral analysis of the emission from the sample. The spectrum was detected by a liquid nitrogen cooled back illuminated CCD camera (Symphony CCD, HORIBA Jobin Yvon) with single photon sensitivity. Images were obtained by scanning the sample (128×128 μm) with a step resolution of 500 nm using the IM 120 scanning stage (Märzhäuser Metzler, Wetzlar-Steindorf, Germany). Raman images were generated by plotting the integrated intensity of the carotenoid Raman band around 1525 cm^{-1} minus fluorescence background as a function of position. Broad-band fluorescence images were constructed by plotting the integrated intensity of fluorescence with superposed Raman bands versus position.

2.4 Statistical analysis

Results are given as mean ± SD.

3 Results

Incubation of HT 29 cells with β-carotene, in the concentration range 0–30 μM, delivered via THF for 24 or 72 h with daily renewal of cell culture medium resulted in an increase in the cellular concentration of β-carotene (Table 1). The highest cellular β-carotene level without any significant cytotoxic effect was observed at 10 μM β-carotene and 72-h incubation (Table 1). Incubation of cells with 10-μM astaxanthin for 72-h did not show any cytotoxic effect either and led to a high cellular uptake of astaxanthin (Table 1). These cell culture conditions (incubation of cells with carotenoids at a concentration of 10-μM for 72-h) were chosen for the following experiments on visualization of carotenoids in HT29 cells.

Table 1. Cellular levels of carotenoids and viability of cells[a)]

Additive	Cellular levels of carotenoids (fmol/cell)		Vitality (%)	
	24-h Incubation	72-h Incubation	24-h Incubation	72-h Incubation
THF (0.5%)	n.d.	n.d.	100 ± 3	100 ± 4
β-Carotene, μM				
3	n.d.	n.d.	97 ± 7	97 ± 3
10	n.d.	8.0 ± 3.5	98 ± 7	97 ± 2
30	3.7 ± 1.5	22.7 ± 10.2	94 ± 3	88.3 ± 2*
THF (0.5%)	n.d.	n.d.	ND	100 ± 3
Astaxanthin, μM				
3	ND	ND	ND	101 ± 2
10	ND	487 ± 22	ND	108 ± 8
30	ND	ND	ND	105 ± 6

a) HT 29 cells were treated with cell culture medium supplemented with either β-carotene or astaxanthin dissolved in THF. Cell culture medium was replaced daily. Cellular levels of carotenoids were estimated after incubation for 24 and 72 h, respectively. Living and metabolically active cells were determined by the MTT test. ND – not determined; n.d. – not detectable; * $p < 0.05$ versus, THF (0.5%)'. Data are presented as mean ± SD.

Figure 1A and B shows weak broad-band fluorescence with superposed Raman bands of 2-mM astaxanthin (Fig. 1A) and 2-mM β-carotene (Fig. 1B) solutions in THF excited at 532-nm. The Raman spectra of astaxanthin and β-carotene are characteristic for carotenoids and contain three intense emission bands around 1000 cm^{-1}, 1155 cm^{-1} and 1525 cm^{-1}. There was no significant detectable background emission of carotenoids in HT 29 cells incubated in medium without carotenoids. Irradiation of astaxanthin-treated cells at 532 nm induced weak broad-band fluorescence with superposed Raman bands, similar to the astaxanthin solution. The Raman spectroscopy image of HT 29 cells incubated with 10 μM astaxanthin for 72 h shows preferential localization of astaxanthin in the cytoplasm (Fig. 2A). The cell nucleus contains a lower amount of astaxanthin. There are some precipitated astaxanthin crystals (Fig. 2A, area 2), which were not removed by washing the cells with PBS. The Raman spectra from different areas of Fig. 2A are shown in Fig. 3, traces 1, 2, 3. The image generated from broad-band fluorescence data shows a similar subcellular distribution of astaxanthin (Fig. 2B).

The cellular concentration of β-carotene detected by HPLC was about 50-fold lower than that of astaxanthin. No detectable Raman bands of β-carotene in cells incubated with 10 μM β-carotene were found, but a weak broad-band fluorescence signal of β-carotene was observed. The broad-

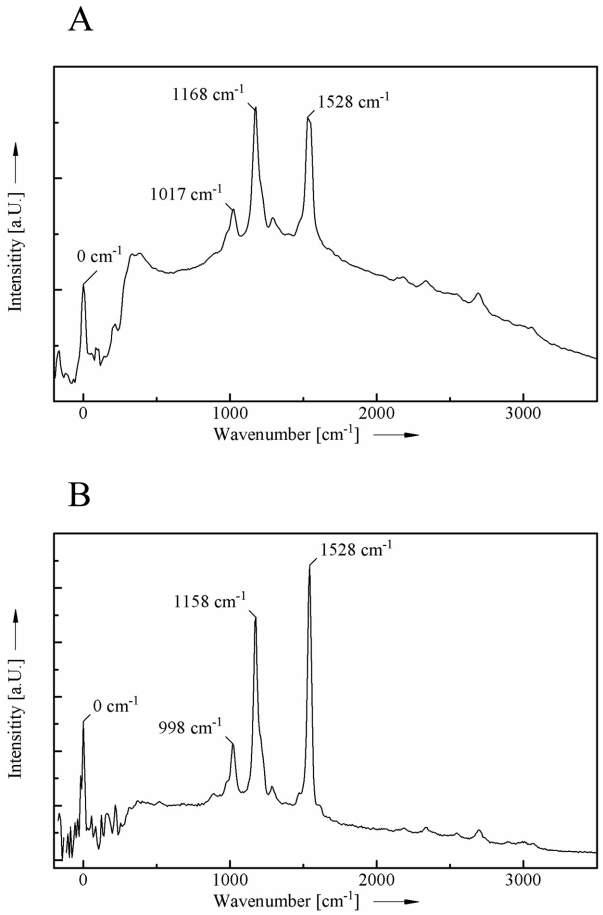

Figure 1. Emission spectra of astaxanthin (A) and β-carotene (B) solutions in THF excited at 532 nm. Carotenoid (2 mM) solution in THF was placed on a microscope slide. The Raman spectra and broad-band fluorescence signal were detected as described in the Section 2.

fluorescence image of β-carotene treated cells is shown in Fig. 4.

4 Discussion

Carotenoids are strong Raman scatterers exhibiting a characteristic Raman spectrum and a strong signal. Measurement of carotenoids in plant tissues by Raman spectroscopy has a long history [15]. During the last 15 years, methods have been developed based on Raman spectroscopy to detect carotenoids in the human skin and retina [16, 17]. Using Raman microspectroscopy the distribution of a carotenoid, β-carotene, in single cells such as human lymphocytes or bovine luteal cells has been investigated [18–20]. In accord with our observations, high amounts of carotenoids at specific sites in the cytoplasm, *e.g.* the Gall bodies, of T lymphocytes and NK cells but not in the nucleus [18, 19] have been found. In bovine luteal cells β-carotene could be detected throughout the volume of the cell, but was predominantly localized in lipid-rich cell components such as the microsomal fraction [20]. It is known that cytoplasm contains less free water than the nucleus, and this might lead to increased accumulation of hydrophobic compounds, like carotenoids, in the cytoplasm. Furthermore, it has been reported that in the intestinal cells (*e.g.* Caco-2 cells) carotenoid inclusion in chylomicrons takes place in the cytoplasm [21].

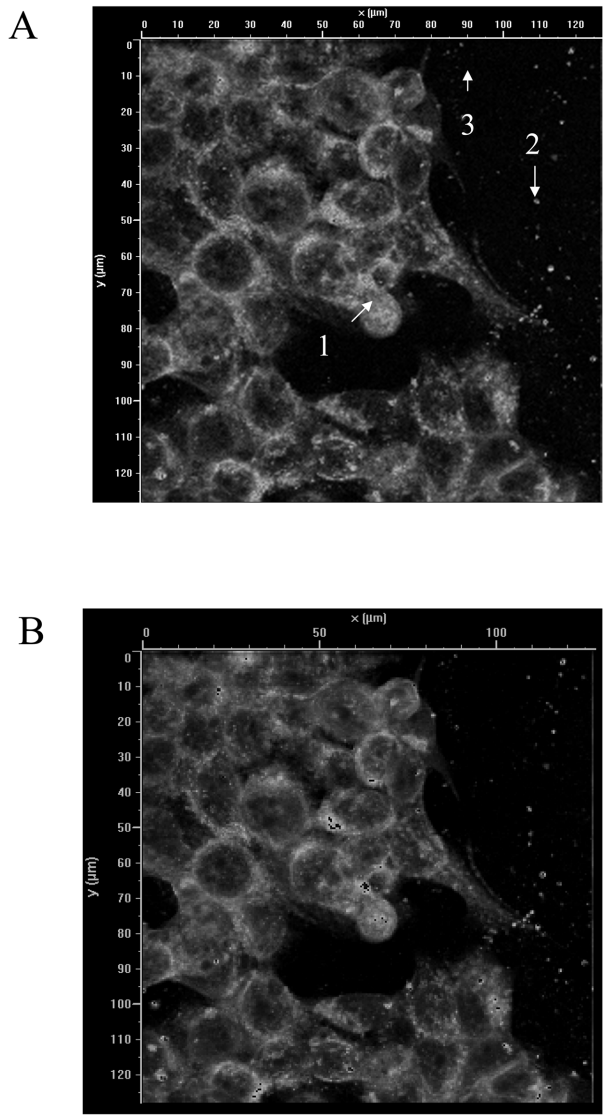

Figure 2. Raman image (A) and broad-band fluorescence image (B) of astaxanthin in intestinal HT 29 cells. Three days after seeding, the cells were incubated with 10 µM astaxanthin for 72 h. Astaxanthin was dissolved in THF. The final concentration of THF in the culture medium was 0.5% v/v. The Raman spectra and broad-band emission spectra were detected as described in Section 2. The image size is (128 × 128 µm).

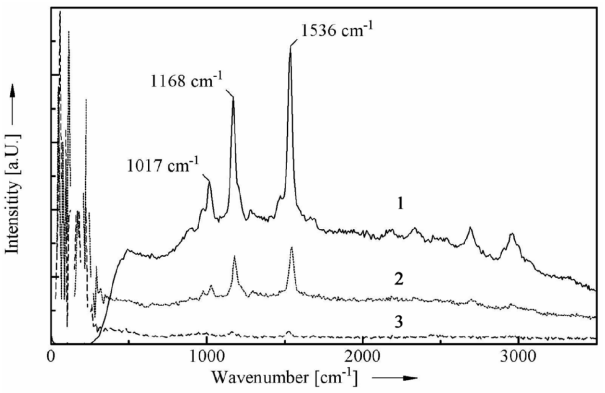

Figure 3. Emission spectra of HT 29 cells treated with astaxanthin. Conditions as in Fig. 2. The spectra were detected as described in Section 2. Trace 1 is Raman spectrum from area 1 (see Fig. 2), trace 2 from area 2, trace 3 from area 3.

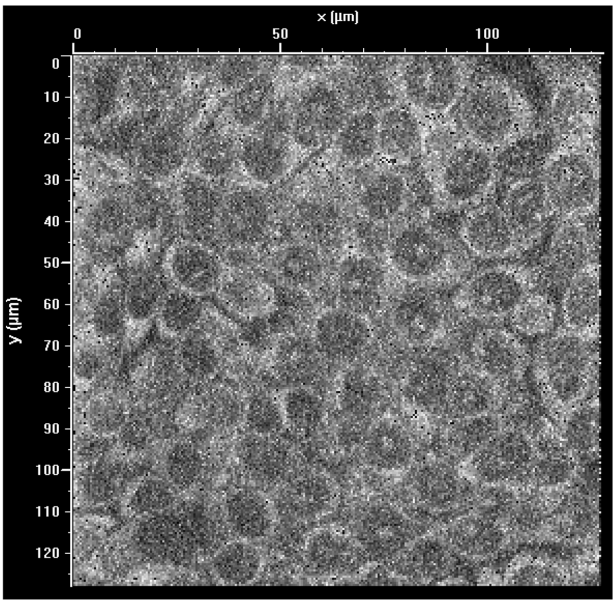

Figure 4. Broad-band fluorescence image of β-carotene in intestinal HT 29 cells. Three days after seeding the cells were incubated with 10 µM β-carotene for 72 h. β-Carotene was dissolved in THF to achieve a final solvent concentration of 0.5% v/v in the culture medium. The broad-band fluorescence spectra were detected as described in Section 2. The image size is (128 × 128 µm).

In addition to Raman imaging we generated images from broad-band astaxanthin and β-carotene fluorescence. It is widely believed that carotenoids are non-fluorescent, but by using HPLC combined with sensitive fluorescent spectrometers it was possible to determine the fluorescence signal of carotenoids. The low quantum yield of carotenoid fluorescence is in the order of 10^{-4} to 10^{-5} [22]. While most carotenoid fluorescence originates from the $S_2 \rightarrow S_0$ transition, β-carotene and fucoxanthin exhibit fluorescence that originates from the $S_1 \rightarrow S_0$ transition [23]. We used carotenoid broad-band fluorescence to generate the image of carotenoid subcellular distribution. Both approaches, broad-band fluorescence and Raman microspectrometry, showed a very similar subcellular distribution of astaxanthin. The concentration of β-carotene was too low to generate a Raman image while a broad-band fluorescence image showed a similar subcellular distribution to that of astaxanthin. It appears that the broad-band fluorescence image approach is more sensitive and better at detecting β-carotene in cells, due to inclusion of emission from a much broader spectrum of wave numbers than that used for Raman microimaging. However, broad-band fluorescence is not as specific as Raman microspectroscopy in complex *in vivo* systems, which might contain a number of unknown compounds with fluorescence properties.

There is a large body of data showing differences in the distribution of carotenoids among organs and tissues. It has been suggested that a high concentration of carotenoids in retina or prostate can effectively protect from reactive molecules. There are differences in the subcellular distribution of carotenoids and, consequently differences in the efficacy with which they protect subcellular structures from damage caused by reactive species such as singlet oxygen or triplet excited species. Additionally, it is possible that the subcellular distribution of carotenoids differ in different cell types, *e.g.* lymphocytes and colon adenocarcinoma cells. In conclusion, this work calls attention to the heterogeneity of astaxanthin subcellular distribution in cells of intestinal origin indicating also heterogeneity of the possible defense against reactive molecules by carotenoids in these cells.

Supported by the Federal Ministry of Consumer Protection, Food and Agriculture, Germany. We gratefully acknowledge the excellent technical assistance of C. Hodapp.

5 References

[1] Buijsse, B., Feskens, E. J., Schlettwein-Gsell, D., Ferry, M., *et al.*, *Am. J. Clin. Nutr.* 2005, *82*, 879 – 886.

[2] van Poppel, G., *Eur. J. Clin. Nutr.* 1996, *50 Suppl 3*, S57 – 61.

[3] Morris, D. L., Kritchevsky, S. B., Davis, C. E., *JAMA* 1994, *272*, 1439 – 1441.

[4] Sundquist, A. R., Briviba, K., Sies, H., *Methods Enzymol.* 1994, *234*, 384 – 388.

[5] Kennedy, T. A., Liebler, D. C., *J. Biol. Chem.* 1992, *267*, 4658 – 4663.

[6] Gradelet, S., Le Bon, A. M., Berges, R., Suschetet, M., Astorg, P., *Carcinogenesis* 1998, *19*, 403 – 411.

[7] Tanaka, T., Kawamori, T., Ohnishi, M., Makita, H., *et al.*, *Carcinogenesis* 1995, *16*, 2957 – 2963.

[8] Ohgami, K., Shiratori, K., Kotake, S., Nishida, T., *et al*., *Invest Ophthalmol. Vis. Sci.* 2003, *44*, 2694 – 2701.

[9] Chew, B. P., Park, J. S., Wong, M. W., Wong, T. S., *Anticancer Res.* 1999, *19*, 1849 – 1853.

[10] Hix, L. M., Frey, D. A., McLaws, M. D., Osterlie, M., *et al*., *Carcinogenesis* 2005, *26*, 1634 – 1641.

[11] Briviba, K., Schnäbele, K., Schwertle, E., Blockhaus, M., Rechkemmer, G., *Biol. Chem.* 2001, *382*, 1663 – 1668.

[12] During, A., Dawson, H. D., Harrison, E. H., *J Nutr.* 2005, *135*, 2305 – 2312.

[13] Weesie, R. J., Merlin, J. C., de Groot, H. J., Britton, G., *et al*., *Biospectroscopy* 1999, *5*, 358 – 370.

[14] Bornemann, R., Walk-Lauffer, B., Raupach, M., *Photonik* 2005, *4*, 60 – 63.

[15] Gill, D., Kilponen, R. G., Rimai, L., *Nature* 1970, *227*, 743 – 744.

[16] Hata, T. R., Scholz, T. A., Ermakov, I. V., McClane, R. W., *et al*., *J. Invest. Dermatol.* 2000, *115*, 441 – 448.

[17] Gellermann, W., Ermakov, I. V., Ermakova, M. R., McClane, R. W., *et al*., *J. Opt. Soc. Am. A. Opt. Image Sci. Vis.* 2002, *19*, 1172 – 1186.

[18] Puppels, G. J., Garritsen, H. S., Kummer, J. A., Greve, J., *Cytometry* 1993, *14*, 251 – 256.

[19] Ramanauskaite, R. B., Segers-Nolten, G. M. J., de Graw, K. J., Sijtsema, N. M., *et al*., *Pure Appl. Chem.* 1997, *69*, 2131 – 2134.

[20] Arikan, S., Sands, H. S., Rodway, R. G., Batchelder, D. N., *Anim. Reprod. Sci.* 2002, *71*, 249 – 266.

[21] During, A., Hussain, M. M., Morel, D. W., Harrison, E. H., *J Lipid Res.* 2002, *43*, 1086 – 1095.

[22] Gillbro, T., Cogdell, R., *J. Chem. Phys. Lett.* 1989, *158*, 312 – 316.

[23] Andersson, P. O., Bachilo, S. M., Chen, R.-L., Gillbro, T., *J. Chem. Phys.* 1995, *99*, 16199 – 16209.

